

CrossMark
click for updates

Cite this: DOI: 10.1039/c4tb00750f

Received 9th May 2014
Accepted 13th September 2014

DOI: 10.1039/c4tb00750f

www.rsc.org/MaterialsB

Enhanced non-viral gene delivery to human embryonic stem cells *via* small molecule-mediated transient alteration of the cell structure†

Jonathan Yen,^a Lichen Yin^b and Jianjun Cheng^{*ab}

Non-viral gene delivery into human embryonic stem cells (hESCs) is an important tool for controlling cell fate. However, the delivery efficiency remains low due in part to the tight colony structure of the cells which prevents effective exposure towards delivery vectors. We herein report a novel approach to enhance non-viral gene delivery to hESCs by transiently altering the cell and colony structure. (*R*)-(+)-*trans*-4-(1-aminoethyl)-*N*-(4-pyridyl)cyclohexanecarboxamide (Y-27632), a small molecule that inhibits the rho-associated protein kinase pathway, is utilized to induce transient colony spreading which leads to an increased transfection efficiency by 1.5 to 2 folds in a spectrum of non-viral transfection reagents including Lipofectamine 2000 and Fugene HD. After removal of Y-27632 post-transfection, cells can revert back to their normal state and do not show alteration of pluripotency. This approach provides a simple, effective tool to enhance non-viral gene delivery into adherent hESCs for genetic manipulation.

1. Introduction

Human embryonic stem cells (hESC) hold tremendous potential in the field of regenerative medicine largely due to their pluripotency. These cells have the ability to differentiate into endoderm, mesoderm, and ectoderm lineages which compose virtually any cell type in the body. Therefore, genetic manipulation of human embryonic stem cells is an important tool in regenerative medicine. The control and expression of specific genes afforded by gene delivery are valuable not only in efforts to control the stem cell fate, but also to study cell behaviour in differentiation and gene targeting studies.¹ Lentiviral transduction has been established as an effective method for gene delivery to hESCs because of their consistently high transfection

efficiency and capability to maintain a stable transgene expression.² However, virus-based delivery systems pose risks of immunogenicity, insertional mutagenesis, and viral integration into the host system.³ In this regard, non-viral gene delivery, often characterized by its desired biocompatibility and minimal immunogenicity, provides an ideal alternative to viral gene delivery.^{4–16} Nevertheless, non-viral systems applied to human embryonic stem cell colonies are hampered by low transfection efficiency, which limits their applications.^{10,16–18}

The low efficiency is, to some extent, attributed to the distinct physiology of hESCs. hESCs are mildly intrinsically stiff in their structure due to the fact that they grow in tight colonies and in rounded up shapes.¹⁹ Because of such tight two dimensional colonies, cells in the centre are often compressed by the surrounding cells²⁰ and exposure of the centred cells to exogenous materials is greatly limited, which prevents effective internalization of gene delivery materials and thus leads to low transfection efficiency. Such a case has been widely noted in previous gene delivery studies,^{16,21–23} showing that the outer edge of the hESCs have notably higher uptake efficiency. These physical properties of the hESC colony growth pose a large limitation in gene delivery that may not be able to be solved through the material design of the delivery vector. To this end, we are seeking alternative strategies to increase the gene delivery efficiency by manipulating the cellular state and physiology of hESCs.

Considering the colony-forming properties of hESCs that limit non-viral gene delivery, we hypothesized that increasing cell spreading would increase the total surface area for interactions with transfection reagents and thus increase cellular uptake and the gene transfection efficiency. Growing hESCs on stiffer substrates has shown to disperse cells and promote cell spreading;^{24,25} it has also been demonstrated in other cell types that an increase in the substrate stiffness can lead to higher transfection efficiency.²⁶ However, such an approach is infeasible for hESCs cells, mainly because of the sensitive nature of hESCs to their external environment; it has been reported that hESCs grown on stiff substrates will start differentiating.²⁷

^aDepartment of Bioengineering, University of Illinois at Urbana-Champaign, Urbana, Illinois, 61801, USA. E-mail: jianjunc@illinois.edu

^bDepartment of Materials Science and Engineering, University of Illinois at Urbana-Champaign, Urbana, Illinois, 61801, USA

† Electronic supplementary information (ESI) available. See DOI: 10.1039/c4tb00750f

However, these studies indicate that cellular uptake is intrinsic to the stiffness and structure of the cells, and a decrease in membrane tension and contractility would lead to increased cellular spreading²⁸ and stimulate endocytosis.²⁹

Dissociation of hESCs into single cells or small colonies can potentially facilitate cell spreading. However, since hESCs are considered to be in the primed state, they are intolerant to single cell passaging and usually exhibit <1% clonal efficiency due to apoptosis upon cellular detachment and dissociation.³⁰ The Rho-associated kinase (ROCK) inhibitor has been used to diminish dissociation-induced apoptosis, resulting in an increased survival of individual hESCs.³⁰ By pre-treatment of the hESCs with (*R*)-(+)-*trans*-4-(1-aminoethyl)-*N*-(4-pyridyl)cyclohexanecarboxamide (Y-27632), a ROCK inhibitor, at 10 μ M for an hour before single cell dissociation, the cloning efficiency increased to 27%. Cells treated with Y-27632 maintain their pluripotency and morphology for at least 5 passages and are able to differentiate into neural cells.³⁰ Therefore, with an attempt to facilitate hESC spreading without causing apoptosis, we herein used the selective ROCK inhibitor, Y-27632, to alter the cell myosin fibers and mimic the cell structure when grown on a stiffer substrate by inhibiting non-myosin IIA.^{31,32} Y-27632 is also known to decrease the cell-generated tension.³³ We hypothesized that Y-27632 would facilitate the spreading and flattening of hESC colonies on plates due to the decreased membrane tension, which would then increase the surface area exposure to allow a more efficient uptake of gene delivery vectors and promote the gene transfection. A broad spectrum of non-viral gene delivery vectors, including commercially available reagents (Lipofectamine 2000 (LPF), Fugene HD (FHD),

poly-L-lysine (PLL), poly-L-arginine (PLR), and poly-ethyleneimine (PEI)), was evaluated in terms of their transfection efficiencies in the presence or absence of Y-27632. Mechanistic analysis into the effect of Y-27632 on cell spreading, cell uptake properties, and pluripotency of hESCs was also performed. The treatment of hESCs with Y-27632 was demonstrated to significantly increase the transfection efficiency of all the tested materials by 1.5 to 2 folds in hESCs, suggesting an alternative use of Y-27632 as a tool for enhanced non-viral gene delivery (Scheme 1).

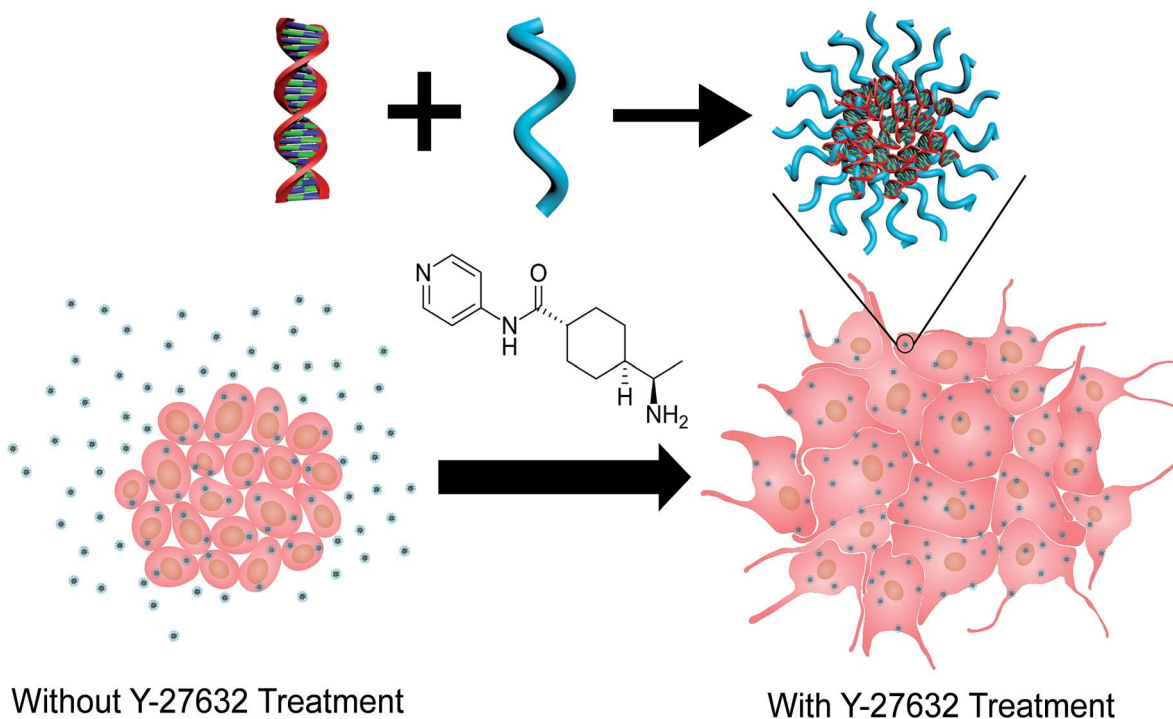
2. Materials and methods

2.1 General

Human embryonic stem cell line H1 (hESC-H1) was cultured in mTeSR 1 medium from Stem Cell Technologies (Vancouver, Canada). FHD was purchased from Promega (Madison, WI, USA). Y-27632 was purchased from Stemgent (Cambridge, MA, USA). Opti-MEM, LPF, and YOYO-1 were purchased from Invitrogen (Carlsbad, CA, USA). pEGFP-N1 was obtained from Elim Biopharmaceuticals (Hayward, CA, USA). Milli-Mark™ Anti-SSEA-4-PE was purchased from EMD Millipore (Billerica, MA, USA). PLL (43 kDa), PLR (7 kDa), and branched PEI (25 kDa) were purchased from Sigma-Aldrich (St Louis, MO, USA).

2.2 Instrumentation

Flow cytometry analysis was conducted on a BD LSRII colour flow cytometer analyser (Becton Dickinson, Franklin Lakes, NJ). Cells were visualized with a Zeiss Axiovert 40 CFL fluorescence



Scheme 1 Y-27632 enhances the transfection efficiencies of various polyplexes or lipoplexes in hESCs *via* increased membrane exposure through transient spreading of the cells.

microscope equipped with a 10 \times and 20 \times objective (Thornwood, NY). Fluorescence imaging was performed using the GE InCell Analyser 2000 from GE Healthcare Sciences (Piscataway, NJ, USA). The zeta potential and size analysis were conducted on a Malvern Zetasizer (Worcestershire, UK).

2.3 Preparation and characterization of nanocomplexes

Various non-viral vectors were used for the transfection analyses. Plasmid DNA (1 μ L, 1 mg mL⁻¹) was diluted with water (50 μ L). The transfection reagent, PLR (10 μ L, 1 mg mL⁻¹), PLL (10 μ L, 1 mg mL⁻¹), or PEI (5 μ L, 1 mg mL⁻¹) was diluted with water (50 μ L). The two solutions were then vortexed gently and allowed to incubate for 20 min at rt, after which they were combined and allowed to incubate for another 20 min at rt.

To prepare LPF/DNA complexes, plasmid DNA (1 μ L, 1 mg mL⁻¹) was diluted with mTeSR (50 μ L). The transfection reagent, LPF (2 μ L, 1 mg mL⁻¹) was diluted with mTeSR (50 μ L). The two solutions were then vortexed gently and allowed to incubate for 20 min at rt, after which they were combined and allowed to incubate for another 20 min at rt.

To prepare FHD/DNA complexes, plasmid DNA (1 μ L, 1 mg mL⁻¹) was diluted with mTeSR (50 μ L). The transfection reagent, FHD (3.5 μ L, 1 mg mL⁻¹) was added to the DNA solution. The solution was then vortexed gently and allowed to incubate for 20 min at rt, after which they were combined and allowed to incubate for another 20 min at rt.

For size and zeta potential assessments, solutions of plasmid DNA (5–25 μ g mL⁻¹) were prepared in water or medium as described above. Separately, a solution of 50 μ g of the vectors was prepared in 400 μ L water. A solution of 50 μ L LPF and FHD in 400 μ L media was also prepared as a control. The DNA solution was then mixed with the vectors, LPF, or FHD solution and allowed to incubate at room temperature for 20 min. Dynamic light scattering (DLS) and zeta potential analysis were conducted on the samples with a Malvern Zetasizer.

2.4 hESC transfection with Y-27632

hESCs were seeded on Matrigel-coated 24-well plates and cultured in mTeSR medium for 24 h. For the full treatment group, Y-27632 was added into the culture medium at a final concentration of 0, 10, 30 or 50 μ M for 4 h prior to transfection. Nanocomplexes prepared from pEGFP-N1 plasmid and different transfection vectors were added dropwise into the media and cells were cultured at 37 $^{\circ}$ C for 4 h. For the pre-treatment group, cells were treated with Y-27632 (50 μ M) for 4 h at 37 $^{\circ}$ C prior to transfection. The cells were then washed with PBS and fresh media were added prior to the addition of the nanocomplex and further incubated at 37 $^{\circ}$ C for 4 h. For the post-treatment group, cells were treated with Y-27632-free medium for 4 h prior to transfection. Directly prior to transfection, the medium was replaced with Y-27632 (50 μ M) containing medium, and cells were transfected with various vectors at 37 $^{\circ}$ C for 4 h. In all these three cases, 4 h after treatment with the nanocomplexes, the media were replaced with fresh mTeSR and cultured for 48 h before measurement of the transfection efficiency by flow cytometry. Alternatively, 10 μ M of

blebbistatin, a non-muscle myosin IIA inhibitor, downstream of the rho-associated protein kinase, was added to the cells prior to and during transfection.

2.5 Intracellular uptake studies

DNA (1 mg mL⁻¹) was labeled with YOYO-1 (20 μ M) at one dye molecule per 50bp of DNA,³⁴ and was allowed to form nanocomplexes with various transfection reagents as described above. hESCs were plated on a matrigel coated 24-well plate and cultured until they reached medium (50 cells) sized colonies. Nanocomplexes were added at 1 μ g YOYO-1-DNA per well and cells were incubated at 37 $^{\circ}$ C for 4 h. Cells were then harvested, re-suspended in PBS, and subjected to flow cytometry analysis to quantify the cellular uptake level of YOYO-1-DNA.

To elucidate the mechanisms underlying the cellular internalization of FHD/DNA nanocomplexes, we performed the uptake study at 4 $^{\circ}$ C or in the presence of various endocytic inhibitors. Cells were pre-treated with chlorpromazine (10 μ g mL⁻¹), genistein (200 μ g mL⁻¹), methyl- β -cyclodextrin (m β CD, 50 μ M), dynasore (80 μ M), or wortmannin (50 nM) for 30 min before the addition of the nanocomplexes and throughout the uptake study at 37 $^{\circ}$ C for 2 h. Results were expressed as percentage uptake level of control cells that were treated with the nanocomplexes at 37 $^{\circ}$ C for 2 h in the presence of Y-27632 (50 μ M) while in the absence of endocytic inhibitors.

2.6 hESC spreading and transfection analysis

hESC H1 were plated on 96-well plates coated with matrigel as medium sized colonies and cultured for 24 h. Y-27632 was added at various concentrations (0, 10, 20, and 50 μ M) and after 4 h incubation, the cell nuclei were stained with Hoechst 33258 and the cytoplasm was stained with CellTracker Red CMTPX per manufacturer's protocols. Forty five fields were imaged using the GE InCell Analyser 2000 in the Hoechst and Texas Red channel (Fig. S1 \dagger). The cytoplasmic area of the cells in each field was quantified using the GE analysis software. The cell spreading level was expressed as the total calculated cytoplasmic area normalized by the number of nucleus counted in the cytoplasmic area (see ESI \dagger for more details).

hESC H1 were seeded on matrigel-coated 24-well plates and cultured in mTeSR medium for 24 h. Before transfection, Y-27632 was added into the culture medium at the final concentration of 0, 10, 30 or 50 μ M, and incubated at 37 $^{\circ}$ C for 4 h. Nanocomplexes from pEGFP-N1 and FHD were added dropwise into the culture medium and cells were further incubated at 37 $^{\circ}$ C for 4 h. The medium was then replaced with fresh mTeSR medium, and cells were further cultured for 48 h. The cell nuclei were stained with Hoechst 33258 and 45 fields were imaged using the GE InCell Analyser 2000 in the Hoechst and GFP channels (Fig. S2 \dagger). The transfection efficiency was then analyzed using the GE InCell Workstation by determining the ratio of GFP positive cells to the number of Hoechst stained nuclei (see ESI \dagger for more details).

2.7 Sample preparation and flow cytometry analysis

Prior to analysis by flow cytometry, transfected cells on the 24-well plate were washed with PBS ($3 \times 500 \mu\text{L}$) to remove any residual serum, dead cells, and debris. Accutase ($100 \mu\text{L}$) was added to detach the cells from the plate, and PBS ($100 \mu\text{L}$) was then added to re-suspend the cells. An aqueous solution of paraformaldehyde (4%, $100 \mu\text{L}$) was added to fix the cells which were then subject to flow cytometry analysis.

2.8 Western blot analysis and SSEA-4 staining

72 h after FHD transfection with $50 \mu\text{M}$ Y-27632 treatment, the cells were stained with DAPI ($250 \mu\text{L}$, 3 nM) and SSEA-4-PE ($250 \mu\text{L}$, 0.02 mg mL^{-1}), a pluripotency cell marker, for 30 min at 37°C . The cells were imaged using the GE InCell Analyser 2000.

After 4 days of treatment of $50 \mu\text{M}$ Y-27632 and FHD transfection, the cells were lysed with the RIPA buffer, mixed with Laemmli buffer supplemented with 2-mercaptoethanol, and heated at 100°C for 5 min to denature the proteins. After being cooled in ice, the samples were subjected to electrophoresis on a 10% SDS PAGE Gel at 120 V for 1.5 h, and wet transferred to the nitrocellulose membrane using the AMRESCO Rapid Western Blot Kit as per manufacturer's instructions. The membrane was stained with OCT4 and α -tubulin primary antibodies and then with HRP-tagged secondary antibodies.

3. Results

3.1 Inhibition of rho-associated kinase facilitates non-viral gene transfection

Prior to the transfection assessment, the pEGFP-N1 plasmid nanocomplexes with the gene transfection vectors were evaluated by dynamic light scattering to determine their complexation capacities. We confirmed that all tested materials were able to form nanocomplexes with DNA as reported by many other prior studies. Upon complexation with DNA, the nanocomplexes of DNA with PLR, PLL and PEI gave sizes around 60–70 nm while DNA complexes with LPF and FHD following the standard protocol afforded a much larger particle size (above 300 nm, Fig. 1a). PLR, PLL, and PEI are cationic polymers with a sufficiently long backbone so that they can well condense the anionic DNA into compact nanocomplexes *via* electrostatic interaction as well as intermolecular entanglement. In comparison, LPF and FHD are cationic lipid based materials, and their short molecular length would prevent sufficient entanglement with the DNA molecules, thus leading to relatively larger complexes.

The transfection efficiency of each material was then evaluated in the presence ($50 \mu\text{M}$) or absence of Y-27632 by monitoring the EGFP expression, attempting to probe the effect of Y-27632 on gene transfection. As shown in Fig. 1b, PLR was unable to mediate transfection in H1 hESCs (transfection efficiency $<1\%$), which was consistent with previous findings in various cell lines.^{4,35} Upon the treatment of Y-27632, all other materials significantly increased the transfection efficiency of hESCs as measured by flow cytometry. Specifically, the PLL transfection efficiency with Y-27632 increased from $3.0 \pm 0.8\%$ to $5.8 \pm 0.8\%$. For PEI mediated transfection, the transfection

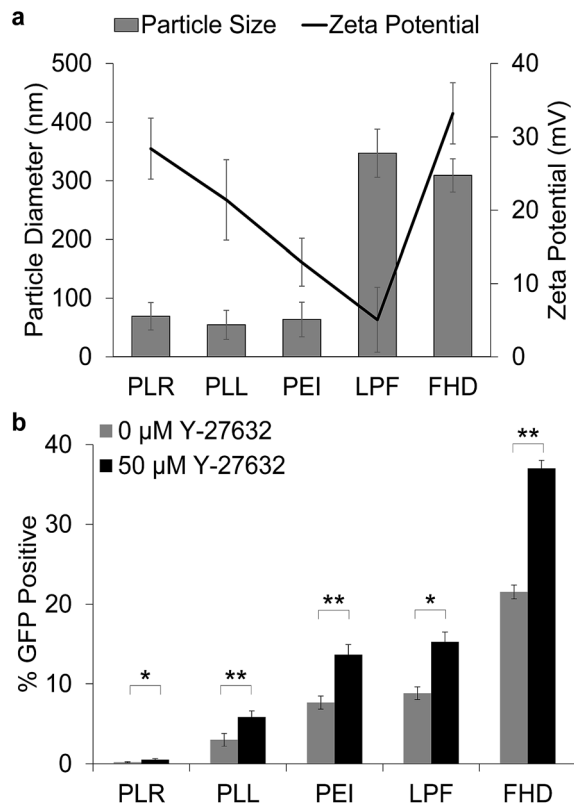


Fig. 1 Y-27632 enhances the transfection efficiencies of various nanocomplexes in hESCs. (a) Size and zeta potential of various nanocomplexes (DNA–polymer, w/w): PLR (1 : 10), PLL (1 : 10), PEI (1 : 5), LPF (1 : 2), and FHD (1 : 3.5). (b) Transfection efficiencies of various reagents in hESCs in the presence ($50 \mu\text{M}$) or absence of Y-27632 as measured by flow cytometry. Cells were pre-treated with Y-27632 cells for 4 h before removal of Y-27632 and addition of various nanocomplexes. ($n = 3$) ($*p < 0.05$, $**p < 0.01$).

efficiency increased from $7.7 \pm 0.8\%$ to $13.7 \pm 1.3\%$ in the presence of Y-27632. Similar enhancement of gene transfection efficiencies were observed with the use of Y-27632 when LPF and FHD were used as transfection agents. Their transfection efficiencies were improved from $8.8 \pm 0.8\%$ to $15.3 \pm 1.2\%$ and $21.5 \pm 0.9\%$ to $37.0 \pm 1.0\%$, respectively. These studies clearly demonstrate that Y-27632 treatment can universally increase the transfection efficiency by approximately 1.7 to 1.9 fold in non-viral gene delivery to hESCs.

3.2 Increased cell spreading by Y-27632 treatment

To further investigate the treatment effect of Y-27632, transfection studies were performed on H1 hESC colonies that were treated with varying concentrations of Y-27632 for 4 h prior to and during transfection. DNA/FHD complexes, which demonstrated the highest transfection efficiency among all tested systems, were selected for further studies. With no treatment, the EGFP transfection efficiency was $14.4 \pm 0.9\%$. With $10 \mu\text{M}$ treatment of Y-27632, the transfection efficiency increased to $17.6 \pm 1.4\%$. When the concentration of Y-27632 was increased to $30 \mu\text{M}$ and $50 \mu\text{M}$, the respective efficiency was increased to $22.7 \pm 0.8\%$ and $26.4 \pm 1.1\%$ (Fig. 2a and b). To confirm that the

mechanism of increased transfection efficiency was due to the spreading and actin–myosin interactions, we treated the cells with blebbistatin, a small molecule that acts downstream of Y-27632,³⁶ inhibits non-muscle myosin IIA, reduces actin–myosin interactions and alters the intracellular structure and morphology. Treatment of blebbistatin at 10 μM also resulted in an increased transfection efficiency of the DNA/FHD complex up to $17.8 \pm 0.4\%$, indicating a strong correlation between the cell structure and the transfection efficiency (Fig. 2a).

When hESC colonies were treated with Y-27632 for 4 h at varying concentrations (10, 30, and 50 μM), significant morphological changes of the cells were observed. In the absence of Y-27632, the cells maintained a two dimensional cobble stone like colony morphology, and the cells were tight and rounded up (Fig. 2c). At 10 μM , the colonies started to spread and lose their rounded-up structure. At 30 and 50 μM , the cells were even more spread out and elongated, indicating that they had relaxed their original structure. This increased the surface area and decreased the surface membrane tension. To further verify the Y-27632-mediated cell spreading, the cytoplasm and nuclei of the Y-27632-treated cells were respectively labelled before cells were imaged and analysed using the GE InCell Analyzer (Fig. S1†). Without Y-27632 treatment, the cells were calculated to have a cytoplasmic area of $445 \pm 29.8 \mu\text{m}^2$ per cell. When treated with Y-27632 at 10, 30, and 50 μM , the cytoplasmic area per cell increased to 516 ± 8.0 , 563 ± 32.7 and $589 \pm 18.6 \mu\text{m}^2$, respectively (Fig. 2d). The increased

cytoplasmic area thus substantiated the promotion of cell spreading upon Y-27632 treatment. Through further analysis of the cell spreading effect on the transfection efficiency, the GFP efficiency was also measured using the GE InCell Analyzer and an InCell Workstation (Fig. S2†). With the increased spreading, the GFP transfection efficiency increases from about $6.3 \pm 3.4\%$ at 0 μM to $10.9 \pm 4.4\%$, $22.8 \pm 0.6\%$ and $30.6 \pm 1.7\%$ at 10, 30, and 50 μM of Y-27632 treatment, respectively (Fig. 2d). Through the GE InCell imaging analysis of the hESCs cytoplasmic area and GFP expression, the correlation between the cell spreading and GFP transfection upon the treatment of Y-27632 was noted.

3.3 Sequential treatment of Y-27632 and uptake inhibition study

To study the importance of morphological changes, hESCs were treated with Y-27632 in three different stages, with FHD as the model vector. When the cells were treated with Y-27632 for 4 h and removed before transfection, the transfection efficiency was $28.9 \pm 1.8\%$. When the cells were treated with Y-27632 only during the transfection for 4 h, the transfection efficiency decreased to $25.4 \pm 1.9\%$. Finally, when the cells were treated for 4 h before and during the transfection with Y-27632, the transfection efficiency increased to $31.3 \pm 3.6\%$ (Fig. 3a). The increase in transfection when the hESCs were pretreated with Y-27632 indicates the importance of altering the cell morphology before the transfection.

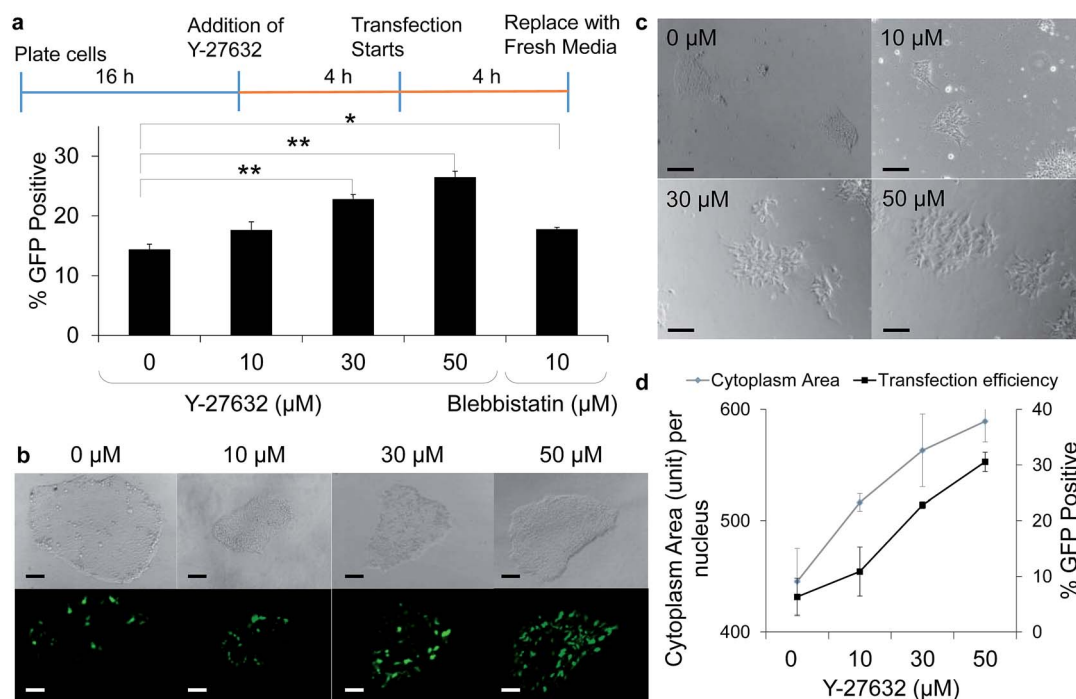


Fig. 2 Y-27632 promotes transfection in hESCs cells by extending the cell surface area. (a) Transfection efficiencies of FHD/DNA nano-complexes in H1 hESCs in the presence of Y-27632 or blebbistatin at various concentrations. (b) Fluorescence images of H1 hESCs 48 h post transfection with FHD/pEGFP nanocomplexes. Cells were pre-treated with 0 μM , 10 μM , 30 μM , or 50 μM Y-27632 for 4 h before transfection and during the 4 h transfection process (scale bar = 250 μm). (c) Bright-field imaging showing the morphological change of hESCs after 4 h treatment with Y-27632 at various concentrations (scale bar = 250 μm). (d) Alteration of the cytoplasm area (μm^2) per nucleus of hESCs following treatment with Y-27632 of various concentrations. Images were taken and analysed with the GE InCell Analyzer. ($n = 5$) (* $p < 0.05$, ** $p < 0.01$).

An uptake study of the YOYO-1-DNA was also conducted in the presence of various concentrations of Y-27632. In the absence of Y-27632, the fluorescence unit of the FHD/YOYO-1-DNA nanocomplexes in the cells was found to be 56.9 ± 2.1 . When the concentration of Y-27632 was increased from 10 to 50 μM , the uptake level continued to increase up to 84.4 ± 0.7 fluorescence unit in the case of 50 μM Y-27632 treatment, which was consistent with the trend of transfection efficiency enhancement (Fig. 3b).

3.4 Treatment of Y-27632 maintains pluripotency of hESCs

Treatment of hESCs with Y-27632 at the concentration of 50 μM significantly increases the non-viral transfection efficiency. The treated cells can also revert back to their normal hESC morphology 48 h post-treatment (Fig. 2b). This study demonstrates that Y-27632 only transiently alters the hESC morphology to facilitate improved gene delivery. To further confirm whether the hESCs were only transiently altered by the treatment of Y-27632 and FHD transfection, extracellular stage specific embryonic antigen 4 (SSEA-4) was stained with PE conjugated antibodies and imaged 72 h post-transfection with 50 μM Y-27632 treatment (Fig. 4a). The cells were stained uniformly positive for SSEA-4, indicating well maintained pluripotency. A western blot assay of the hESCs conducted 4 days post FHD/DNA transfection with Y-27632 also demonstrated an unaltered expression of OCT4, a gene indicator of hESC pluripotency. With the treatment of Y-27632 at all concentrations, there was no change in the OCT4 expression. However, when treated with 10, 30, and 50 μM of Y-27632 in the presence of

a EGFP Transfection Efficiency Dependence on the Presence of Y-27632 either before and/or during the Transfection Step

| Pre-incubation (4h) | Transfection (4 h) | % GFP Positive |
|---------------------|--------------------|----------------|
| --- | --- | 19.6 ± 0.8 |
| --- | 50 μM | 25.4 ± 1.9 |
| 50 μM | --- | 28.9 ± 1.8 |
| 50 μM | 50 μM | 31.3 ± 3.6 |

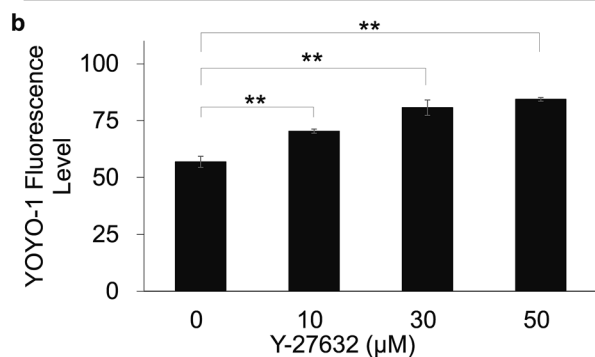


Fig. 3 Y-27632 promotes cellular internalization of the gene cargo as a result of increased surface area. (a) Transfection efficiency of FHD in hESCs in the presence of Y-27632. Y-27632 was applied to the cells for 4 h before transfection, during the 48 h transfection period, or a combination thereof. (b) Cell uptake level of FHD/YOYO-1-DNA nanocomplexes in hESCs in the presence of various concentrations of Y-27632 ($n = 3$). ($*p < 0.05$, $**p < 0.01$).

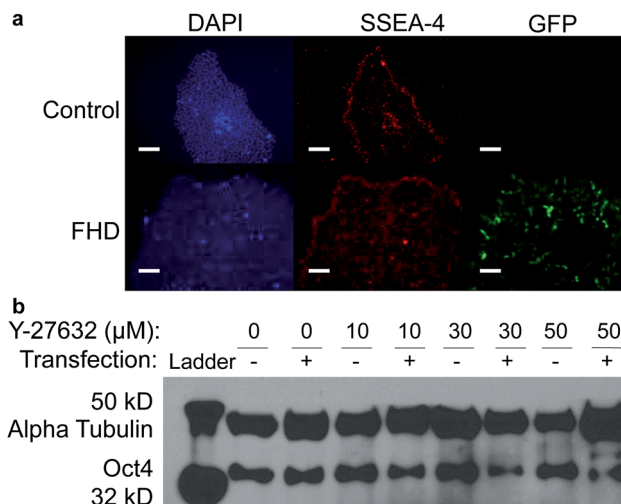


Fig. 4 Y-27632 does not compromise the pluripotency of H1 hESCs. (a) DAPI and SSEA-4 staining patterns of H1 hESCs without Y-27632 treatment (control group) or transfected with FHD in the presence of 50 μM Y-27632 (FHD group, scale bar = 250 μm). (b) Western blot analysis on the OCT4 expression in hESCs 4 days post FHD transfection and treatment of Y-27632 at various concentrations. (– demonstrates the cells without transfection and + indicates cells with FHD transfection).

FHD, slight reduction in the OCT4 expression level was observed, indicating that Y-27632 itself did not affect pluripotency and the minor change of the OCT4 expression could be induced by the transfection reagent. These experiments substantiated that gene transfection and Y-27632 treatment were transient and the cells were able to revert back to their natural pluripotent state after removal of Y-27632 (Fig. 4b). The treatment of hESCs with Y-27632 also showed no cytotoxicity to the cells at any treatment concentrations (Fig. S3[†]). The Y-27632 treatment at any of the concentrations for transfection demonstrated only transient alteration of the cells with well retained pluripotency and low cytotoxicity.

4. Discussion

In the current study, we demonstrated that with the treatment of Y-27632, transfection efficiencies of a variety of non-viral gene delivery materials in hESC, including PLR, PLL, PEI, LPF, and FHD, were markedly augmented. Y-27632 allowed the hESC colonies to effectively transform their internal mechanical structure by inhibiting the actin-myosin contractility and cell-to-cell adhesion, thus facilitating spreading of the cells. As such, the exposed surface area was increased and the membrane tension was decreased, ultimately leading to an increase in the internalization level of exogenous genetic materials. Using one of the most efficient commercial transfection reagents, FHD, we demonstrated a dose dependent effect of Y-27632 small molecule treatment on hESCs. An increase in the Y-27632 concentration from 0 to 50 μM correlated to a 1-fold increment in the transfection efficiency. To ensure that the increased transfection efficiency was due to the actin-myosin inhibition effect

on the spreading or morphology change of the cells and not the other pathways associated with the rho-associated protein kinase pathway, the cells were also treated with 10 μM blebbistatin. Blebbistatin acts downstream of the rho-associated protein kinase, and directly inhibits non-muscle myosin IIA. This inhibition directly decreases the affinity of myosin with actin, indicating that the role of Y-27632 in the cell morphological change is responsible for the increased gene transfection.

From the treatment of varying concentrations of Y-27632, the morphology of cells changed from a rounded up structure to an elongated flat morphology and disassociation from the colony was observed. This flattening and spreading of the cells increased the cell surface area that was exposed to exogenous nano-complexes, and thus the nanocomplexes could be more readily taken up by the cells. A higher Y-27632 concentration resulted in enhanced cell spreading and ultimately increased the transfection efficiency. The important role of Y-27632 in increasing cell adhesion and survival also helped the cells to maintain physiological functions, thus contributing to the transfection process.²⁴ In addition, through the spreading and elongation of the cells, the cell membrane could also have decreased membrane tension, allowing a higher rate of endocytosis.^{28,29}

It is important that the cells be transiently altered before transfection, such that spreading of the cells and decrease of the membrane tension could allow efficient nanocomplex uptake. In our detailed study on the adding sequence of Y-27632, pre-treated cells showed a significantly higher transfection efficiency than post-treated cells, indicating the importance of morphological changes prior to the transfection process. The altered morphology primes the cells by increasing the cytoplasmic area and facilitating the uptake of the nano-complexes during transfection. In consistence with our findings that cells in smaller colonies afforded higher transfection efficiencies (data not shown), it was further demonstrated that Y-27632-mediated cell spreading and a larger cell surface area were attributed to the decreased surface tension and declumping of the cell colonies. As previously reported,³⁰ the use of Y-27632 does not permanently affect the pluripotency and hESC cell state. In accordance with such a finding, the cells recovered to their natural, tight, two-dimensional colony morphology 72 h after removal of Y-27632. Expressions of SSEA-4 and OCT4 were also observed, suggesting reversible alteration of cell physiology and maintenance of cell pluripotency.

5. Conclusions

We studied and adapted a new approach to increase the non-viral gene delivery to hESCs by transiently altering the colony structure to increase their susceptibility for uptake of nano-complexes. Treatment of hESCs with Y-27632 prior to and during transfections effectively increases cell spreading and decreases cell membrane tension, which increases cell uptake and thus potentiates the gene transfection. The hESCs colonies were able to return to their original morphology and maintain their pluripotency within hours after removal of Y-27632. While most of the current studies in non-viral gene delivery focus on the material design, this study opens a new window to control

gene transfection in hESCs on the cellular side. It therefore provides a promising approach to manipulate pluripotent stem cells through transient gene therapy, overcoming a big hurdle against controlling and studying pluripotent stem cell differentiation and development toward various biomedical applications. With the increase in the gene transfection efficiency, an increase in differentiation efficiency of hESCs can be expected, which would reduce the need for enrichment and sorting of the desired cells. The preliminary findings of the current study also unravel the possibility to manipulate the cellular states and properties in future designs of intracellular delivery vehicles into hESCs.

Acknowledgements

This work is supported by NIH (Director's New Innovator Award 1DP2OD007246 and 1R21EB013379 for J.C) and NSF (CHE 1153122). J.Y. was funded at UIUC from National Science Foundation (NSF) Grant 0965918 IGERT: Training the Next Generation of Researchers in Cellular and Molecular Mechanics and BioNanotechnology. The authors thank Dr. Fei Wang for his support and discussion.

Notes and references

- 1 J. Zou, M. L. Maeder, P. Mali, S. M. Pruetz-Miller, S. Thibodeau-Beganny, B. K. Chou, G. Chen, Z. Ye, I. H. Park, G. Q. Daley, M. H. Porteus, J. K. Joung and L. Cheng, Gene targeting of a disease-related gene in human induced pluripotent stem and embryonic stem cells, *Cell Stem Cell*, 2009, 5(1), 97–110.
- 2 Z. Ye, X. Yu and L. Cheng, Lentiviral gene transduction of mouse and human stem cells, *Methods Mol. Biol.*, 2008, 430, 243–253.
- 3 U. P. Dave, N. A. Jenkins and N. G. Copeland, Gene therapy insertional mutagenesis insights, *Science*, 2004, 303(5656), 333.
- 4 L. Yin, Z. Song, K. H. Kim, N. Zheng, H. Tang, H. Lu, N. Gabrielson and J. Cheng, Reconfiguring the architectures of cationic helical polypeptides to control non-viral gene delivery, *Biomaterials*, 2013, 34(9), 2340–2349.
- 5 K. W. Leong, H. Q. Mao, V. L. Truong-Le, K. Roy, S. M. Walsh and J. T. August, DNA-polycation nanospheres as non-viral gene delivery vehicles, *J. Controlled Release*, 1998, 53(1–3), 183–193.
- 6 K. Kizjakina, J. M. Bryson, G. Grandinetti and T. M. Reineke, Cationic glycopolymers for the delivery of pDNA to human dermal fibroblasts and rat mesenchymal stem cells, *Biomaterials*, 2012, 33(6), 1851–1862.
- 7 P. M. McLendon, K. M. Fichter and T. M. Reineke, Poly(glycoamidoamine) Vehicles Promote pDNA Uptake through Multiple Routes and Efficient Gene Expression via Caveolae-Mediated Endocytosis, *Mol. Pharm.*, 2010, 7(3), 738–750.
- 8 S. Srinivasachari and T. M. Reineke, Versatile supramolecular pDNA vehicles via click polymerization of

- beta-cyclodextrin with oligoethyleneamines, *Biomaterials*, 2009, **30**(5), 928–938.
- 9 F. Yang, S. W. Cho, S. M. Son, S. R. Bogatyrev, D. Singh, J. J. Green, Y. Mei, S. Park, S. H. Bhang, B. S. Kim, R. Langer and D. G. Anderson, Genetic engineering of human stem cells for enhanced angiogenesis using biodegradable polymeric nanoparticles, *Proc. Natl. Acad. Sci. U. S. A.*, 2010, **107**(8), 3317–3322.
- 10 F. Yang, J. J. Green, T. Dinio, L. Keung, S. W. Cho, H. Park, R. Langer and D. G. Anderson, Gene delivery to human adult and embryonic cell-derived stem cells using biodegradable nanoparticulate polymeric vectors, *Gene Ther.*, 2009, **16**(4), 533–546.
- 11 M. S. Shim and Y. J. Kwon, Controlled delivery of plasmid DNA and siRNA to intracellular targets using ketalized polyethylenimine, *Biomacromolecules*, 2008, **9**(2), 444–455.
- 12 M. S. Shim and Y. J. Kwon, Acid-transforming polypeptide micelles for targeted nonviral gene delivery, *Biomaterials*, 2010, **31**(12), 3404–3413.
- 13 M. S. Shim and Y. J. Kwon, Dual mode polyspermine with tunable degradability for plasmid DNA and siRNA delivery, *Biomaterials*, 2011, **32**(16), 4009–4020.
- 14 X. A. Jiang, Y. R. Zheng, H. H. Chen, K. W. Leong, T. H. Wang and H. Q. Mao, Dual-Sensitive Micellar Nanoparticles Regulate DNA Unpacking and Enhance Gene-Delivery Efficiency, *Adv. Mater.*, 2010, **22**(23), 2556–2560.
- 15 N. P. Gabrielson, H. Lu, L. C. Yin, D. Li, F. Wang and J. J. Cheng, Reactive and Bioactive Cationic α -Helical Polypeptide Template for Nonviral Gene Delivery, *Angew. Chem., Int. Ed.*, 2012, **51**(5), 1143–1147.
- 16 J. Yen, Y. F. Zhang, N. P. Gabrielson, L. C. Yin, L. N. Guan, I. Chaudhury, H. Lu, F. Wang and J. J. Cheng, Cationic, helical polypeptide-based gene delivery for IMR-90 fibroblasts and human embryonic stem cells, *Biomater. Sci.*, 2013, **1**(7), 719–727.
- 17 J. J. Green, B. Y. Zhou, M. M. Mitalipova, C. Beard, R. Langer, R. Jaenisch and D. G. Anderson, Nanoparticles for Gene Transfer to Human Embryonic Stem Cell Colonies, *Nano Lett.*, 2008, **8**(10), 3126–3130.
- 18 N. Kobayashi, J. D. Rivas-Carrillo, A. Soto-Gutierrez, T. Fukazawa, Y. Chen, N. Navarro-Alvarez and N. Tanaka, Gene delivery to embryonic stem cells, *Birth Defects Res., Part C*, 2005, **75**(1), 10–18.
- 19 J. A. Thomson, J. Itskovitz-Eldor, S. S. Shapiro, M. A. Waknitz, J. J. Swiergiel, V. S. Marshall and J. M. Jones, Embryonic stem cell lines derived from human blastocysts, *Science*, 1998, **282**(5391), 1145–1147.
- 20 K. E. Hammerick, Z. B. Huang, N. Sun, M. T. Lam, F. B. Prinz, J. C. Wu, G. W. Commons and M. T. Longaker, Elastic Properties of Induced Pluripotent Stem Cells, *Tissue Eng., Part A*, 2011, **17**(3–4), 495–502.
- 21 C. Xiong, D. Q. Tang, C. Q. Xie, L. Zhang, K. F. Xu, W. E. Thompson, W. Chou, G. H. Gibbons, L. J. Chang, L. J. Yang and Y. E. Chen, Genetic engineering of human embryonic stem cells with lentiviral vectors, *Stem Cells Dev.*, 2005, **14**(4), 367–377.
- 22 X. Xia, Y. Zhang, C. R. Ziegler and S. C. Zhang, Transgenes delivered by lentiviral vector are suppressed in human embryonic stem cells in a promoter-dependent manner, *Stem Cells Dev.*, 2007, **16**(1), 167–176.
- 23 X. Xia and S. C. Zhang, Genetic modification of human embryonic stem cells, *Biotechnol. Genet. Eng. Rev.*, 2007, **24**, 297–309.
- 24 N. Harb, T. K. Archer and N. Sato, The Rho-Rock-Myosin Signaling Axis Determines Cell-Cell Integrity of Self-Renewing Pluripotent Stem Cells, *PLoS One*, 2008, **3**(8), e3001.
- 25 J. N. Lakins, A. R. Chin and V. M. Weaver, Exploring the link between human embryonic stem cell organization and fate using tension-calibrated extracellular matrix functionalized polyacrylamide gels, in *Progenitor cells*, Springer, 2012.
- 26 H. J. Kong, J. D. Liu, K. Riddle, T. Matsumoto, K. Leach and D. J. Mooney, Non-viral gene delivery regulated by stiffness of cell adhesion substrates, *Nat. Mater.*, 2005, **4**(6), 460–464.
- 27 J. Zoldan, E. D. Karagiannis, C. Y. Lee, D. G. Anderson, R. Langer and S. Levenberg, The influence of scaffold elasticity on germ layer specification of human embryonic stem cells, *Biomaterials*, 2011, **32**(36), 9612–9621.
- 28 D. Raucher and M. P. Sheetz, Cell spreading and lamellipodial extension rate is regulated by membrane tension, *J. Cell Biol.*, 2000, **148**(1), 127–136.
- 29 J. Dai and M. P. Sheetz, Regulation of endocytosis, exocytosis, and shape by membrane tension, *Cold Spring Harbor Symp. Quant. Biol.*, 1995, **60**, 567–571.
- 30 K. Watanabe, M. Ueno, D. Kamiya, A. Nishiyama, M. Matsumura, T. Wataya, J. B. Takahashi, S. Nishikawa, S. Nishikawa, K. Muguruma and Y. Sasai, A ROCK inhibitor permits survival of dissociated human embryonic stem cells, *Nat. Biotechnol.*, 2007, **25**(6), 681–686.
- 31 R. Kaunas, P. Nguyen, S. Usami and S. Chien, Cooperative effects of Rho and mechanical stretch on stressfiber organization, *Proc. Natl. Acad. Sci. U. S. A.*, 2005, **102**(44), 15895–15900.
- 32 R. McBeath, D. M. Pirone, C. M. Nelson, K. Bhadriraju and C. S. Chen, Cell shape, cytoskeletal tension, and RhoA regulate stem cell lineage commitment, *Dev. Cell*, 2004, **6**(4), 483–495.
- 33 S. Narumiya, T. Ishizaki and M. Uehata, Use and properties of ROCK-specific inhibitor Y-27632, *Regulators and Effectors of Small Gtpases, Pt D*, 2000, **325**, 273–284.
- 34 N. P. Gabrielson and J. J. Cheng, Multiplexed supramolecular self-assembly for non-viral gene delivery, *Biomaterials*, 2010, **31**(34), 9117–9127.
- 35 H. Y. Tang, L. C. Yin, K. H. Kim and J. J. Cheng, Helical poly(arginine) mimics with superior cell-penetrating and molecular transporting properties, *Chem. Sci.*, 2013, **4**(10), 3839–3844.
- 36 M. Ohgushi, M. Matsumura, M. Eiraku, K. Murakami, T. Aramaki, A. Nishiyama, K. Muguruma, T. Nakano, H. Suga, M. Ueno, T. Ishizaki, H. Suemori, S. Narumiya, H. Niwa and Y. Sasai, Molecular pathway and cell state responsible for dissociation-induced apoptosis in human pluripotent stem cells, *Cell Stem Cell*, 2010, **7**(2), 225–239.